Arch. Metall. Mater. **69** (2024), 1, 197-208

DOI: https://doi.org/10.24425/amm.2024.147809

HAO XU[1], RUI-BIN GOU[1*], MIN YU[2], WEN-JIAO DAN[1], NIAN WANG[3]

THE INFLUENCE OF SHORT-TERM HIGH TEMPERATURE ENVIRONMENT ON THE NON-UNIFORM DISTRIBUTION OF FERRITE GRAIN SIZE IN 40 MM-THICK Q345 STEEL

In order to reveal the non-uniform distribution of grain size in thick direction for engineering heavy plate, microstructure of 40 mm-thick Q345 steel was observed and measured under different short-term high temperature environments formed by fire. Moreover, the influence of the short-term high temperature environment was revealed on the distribution of ferrite grain size in the Q345 steel. Under different fire service environments, there was a log-normal distribution relationship between the distribution parameter N_f (number of ferrite grains) and d_f (average grain diameter), as well as ρ_{Af} (area fraction density) and d_f, at different positions along the thickness direction. However, the statistical results are greatly affected by the length of the statistical interval. When d_f is about 4 to 6 times the length of the statistical interval, the statistical accuracy is higher. By using nonlinear fitting method, multiple non-uniform distribution empirical models including N_f-d_f empirical formulas and ρ_{Af}-d_f empirical formulas were established at different positions along thick direction under various fire environments. Furthermore, the interrelationships between fire temperature T and N_f, T and ρ_{Af}, fire duration t and N_f, t and ρ_{Af} were revealed, respectively.

Keywords: Short-term high temperature environment; Q345 thick plate; Microstructure; Distribution model

Notation

Notation the following symbols are used in this paper:

- l surface distance,
- L statistical interval length,
- d_i the diameter of ferrite grain,
- d_f the average diameter of ferrite grains within each statistical interval,
- N_f the number percentage of grains within each statistical interval,
- ρ_{Af} the area fraction density of grains within each statistical interval,
- d average diameter.

1. Introduction

Due to the excellent mechanical properties of low alloy structural steel, it is widely used in fields such as machinery and agricultural engineering [1-3]. In recent years, because of the continuous development of engineering steels towards large size, high load-bearing capacity and long service life, the demand and mechanical performance requirements for thick plates have been increasing year by year. However, both the deformation and the rolling temperature differ in the thickness direction during the rolling process of thick plate, and they lead to the non-uniform distribution both of microstructure and mechanical properties [4-5]. Meanwhile, the risk of fire in steel structures has been increasing in extreme environments, and the short-term high temperature environment formed by fire (fire environment) significantly affects microstructure and mechanical properties of the materials [6-7], thus impacts the service safety performance of steel structures. Therefore, conducting research on the variation law of microstructure in engineering thick plates is of great significance for ensuring their service safety performance under the action of short-term high temperature environments.

A great deal of research has been conducted by domestic and foreign scholars on the microstructural distribution of engineering steels [8]. In terms of the relationships between high-temperature service environments and material microstructure [9-15], Zeng et al. studied the variation of microstructure

[1] ANHUI SCIENCE AND TECHNOLOGY UNIVERSITY, COLLEGE OF MECHANICAL ENGINEERING, FENGYANG 233100, ANHUI, CHINA
[2] ANHUI SCIENCE AND TECHNOLOGY UNIVERSITY, COLLEGE OF ARCHITECTURE, BENGBU 233000, CHINA
[3] BENGBU SPECIAL EQUIPMENT SUPERVISION AND INSPECTION CENTER, BENGBU 233000, CHINA

* Correspondence e-mail: rbgou304@163.com

in post-fire 4 mm-thick Q890 steel and found that the fire temperature affects the phase size and the constituent phases in the investigated material [13]. Wang et al. investigated the influence of TMCP process on the microstructure and properties of 20 mm-thick Q460q steel, and found that both the volume fraction and grain size of ferrite are inversely proportional to the rolling temperature [14]. Wu et al. studied the evolution of microstructure in the heat-affected zone of a 1.2 mm-thick Q&P980 steel under different peak temperature conditions, they found there is a single phase of martensitic and the volume percentage of retained austenite decreases from 13% to 2% when the peak temperature increases from 300°C to 1350°C [15]. Regarding the combined effects of high temperature and time on material microstructure [16-19], Liu et al. studied the influence of austenitization temperature and holding time on grain size in 1.5 mm-thick 22MnB5NbV steel, and found that there is a proportional relationship between the grain size and temperature, as well as the grain size and holding time extension [17]. Li et al. investigated the effect of holding time on the microstructure of 1.6 mm-thick B1500HS steel after heating at 930°C, and observed a reduction in the volume fraction of martensite with increasing holding time [18]. Xie et al. studied the influence of holding time on carbide size and distribution in 960 MPa grade low alloy steel, and found that prolonging the holding time leads to the coarsening of carbides [19]. In terms of research on the models and characterization of material grain size distribution [20-23], Yu et al. studied the non-uniformity of microstructure in both 2 and 3 mm-thick DP600 thin plates, and established models for accurately describing the non-uniform distribution of microstructure in thin plate [20]. Kazakov et al. investigated the microstructural non-uniformity of 25-70 mm hot-rolled thick plates and proposed a method to evaluate microstructural anisotropy [21]. Yamashita et al. analyzed the influence of friction stir welding on the non-uniformity of microstructure along the thickness direction in 2 mm dual-phase stainless steel, and revealed the variation of grain size in the α and γ phases along the thickness direction [22]. Virgínia et al. found the non-uniformity of microstructure in quarter and middle thicknesses of 80 mm-thick S690QL high-strength steel and proposed a characterization method for the multiphase microstructure of quenched and tempered high-strength steel [23]. In summary, scholars have paid more attention to the study of microstructural distribution in thin plates, while further research is still needed on the influence of short-term high temperature environments on the grain size distribution of thick plates, especially in terms of non-uniform distribution models in the thickness direction. Therefore, it is of great significance to study the distribution laws of microstructure in thick plates under the action of short-term high temperature environments, which is very important for ensuring their service safety performance.

To reveal the distribution characteristics of microstructure in thick plates under the short-term high temperature environments formed by fire, this study focuses on Q345 thick plate. By simulating the short-term high temperature service environment, the non-uniformity of grain size distribution in Q345 thick plate was investigated under different fire conditions. Firstly, a considerable amount of morphological data of microstructure in the thickness direction of Q345 thick plates was obtained from microscopy observations. Secondly, image processing software was employed to statistically analyze the grain size of ferrite so as to reveal the non-uniform distribution characteristics of grain size in the thickness direction. Thirdly, based on the statistical results, a nonlinear fitting method was utilized to study the mutual relationships between d_f both and N_f and ρ_{Af} to construct non-uniform distribution models of N_f-d_f and ρ_{Af}-d_f, respectively. Finally, based on the established non-uniform distribution models, the influence mechanism of short-term high temperature environment was discussed on the distribution of ferrite grain size in the 40 mm-thick Q345 steel. The research results in this work can provide theoretical guidance for microstructure evaluation and prediction of Q345 thick plate after short-term high-temperature service.

2. Experimental

2.1. Materials and specimens

The experimental material used in this study is Q345 thick steel plate, whose chemical compositions are presented in TABLE 1. Multiple 200 mm (Transverse Direction, TD) × 100 mm (Rolling Direction, RD) × 40 mm (Normal Direction, ND) specimens (Fig. 1a) were taken from the Q345 steel. Subsequently, a 4 mm (TD) × 100 mm (RD) × 25 mm (ND) test piece (Fig. 1b) was obtained from each specimen. The dimensions of the specimen and the test piece are shown in Fig. 1.

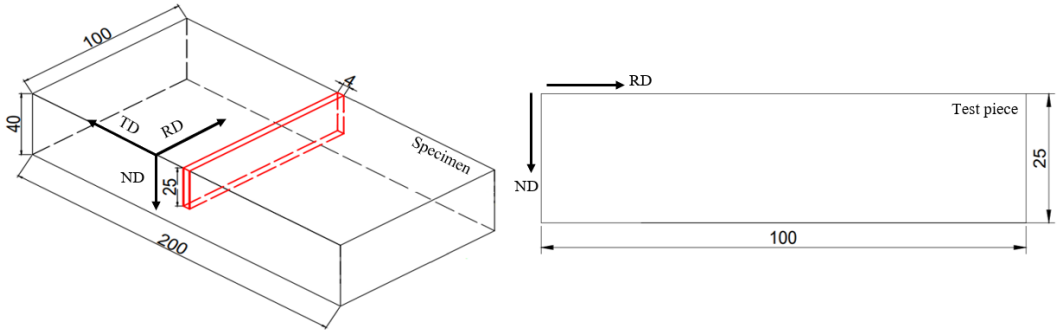

Fig. 1. The dimensions of the specimen and the test piece (a) Specimen (b) Test piece

TABLE 1

Chemical compositions of the 40 mm-thick Q345 steel (wt.%)

C	Si	Mn	P	S	Al	Ti	Ni	Cr	Cu
0.19	0.06	1.10	0.11	0.02	0.20	0.01	0.02	0.04	0.04

2.2. Methods of fire disaster

To elucidate the influence of fire environment on the distribution of ferrite grain size in the investigated Q345 steel, the following procedures were conducted: Firstly, the specimen was placed in a furnace and heated at a rate of 10°C/min to the specified temperature referring to 300°C, 500°C and 700°C, respectively. Secondly, keeping the specimen warm for a certain period of time ranging from 40 min to120 min at the target temperature. Thirdly, the specimen was removed from the furnace and was cooled to room temperature by water. Finally, a test piece was extracted from each fire-treated specimen. Total 9 groups of test pieces were obtained according to above mentioned procedures, and the nine different kinds of post-fire pieces together with the original piece are shown in TABLE 2.

2.3. Scheme of microstructure observation in thickness direction

In order to investigate the distribution characteristics of ferrite grain size in the 40mm-thick Q345 steel plate under different fire environments, there are total 16 observation points on each piece which were evenly divided into four columns along the RD and four rows along the ND, respectively. The location of each observation point was defined by the distance l from the observation point to the surface of the piece. The distances of various measuring points in the four rows are l = 2 mm, l = 10 mm, l = 20 mm and l = 24 mm, respectively. The measuring points and their locations were indicated in Fig. 2.

2.4. Grain distribution parameters of ferrite

To reveal the characteristics of grain size in the investigated 40 mm-thick Q345 steel, Firstly, the total number of ferrite grains N of four observation points in the same row was statistically counted, for example, points #1-1, #2-1, #3-1, #4-1 in the first row with l = 2 mm. Then, image processing software was used to measure the grain area A_i and the grain diameter d_i

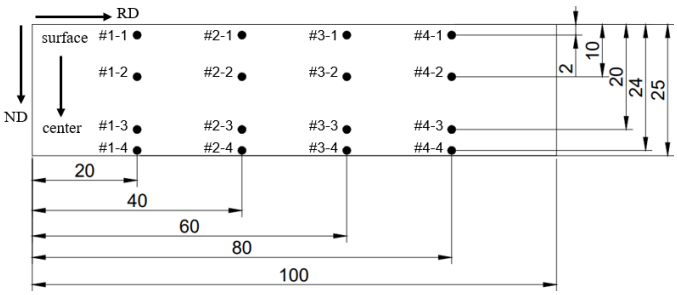

Fig. 2. Diagram of observation point locations

obtained by the method of equivalent circular area, as shown in Equation (1). Thirdly, the obtained grain diameters d_i were divided into different intervals based on the statistical interval length L (L = 3 μm, 5 μm and 10 μm), and the average diameter d_f of ferrite grains within each statistical interval was obtained using Equation (2). Fourthly, the number percentage of ferrite grains within each statistical interval N_f and the area fraction density ρ_{Af} were calculated according to Equations (3) and (4), respectively. Finally, non-linear regression analysis was utilized to describe the non-uniform distribution of grain sizes in Q345 thick plates after fire.

$$d_i = \sqrt{\frac{4A_i}{\pi}} \tag{1}$$

where d_i is the diameter of ferrite grain, μm; A_i is the grain area, μm^2.

$$d_f = \frac{1}{n}\sum d_i \tag{2}$$

where d_f is the average diameter of ferrite grains within each statistical interval, μm; n is the number of grains within each statistical interval.

$$N_f = \frac{n}{N}\times 100\% \tag{3}$$

where N_f is the number percentage of grains within each statistical interval, %; parameters n and N are the number of grains within each statistical interval and the total number of grains in the observed region, respectively.

$$\rho_{Af} = \sum_{i=1}^{n}\frac{1}{A_i} \tag{4}$$

where ρ_{Af} is the area fraction density of grains within each statistical interval, μm^{-2}.

TABLE 2

Groups of the post-fire and the original pieces

Holding time/min / Target temperature/°C	0	40	60	120
20	20°C-0 min	—	—	—
300	—	300°C-40 min	300°C-60 min	300°C-120 min
500	—	500°C-40 min	500°C-60 min	500°C-120 min
700	—	700°C-40 min	700°C-60 min	700°C-120 min

3. Results

3.1. Microstructural observation results of Q345 thick plate

The typical microstructure of different post-fire test pieces is shown in Fig. 3. From Fig. 3, microstructure of the employed Q345 thick plate consists of pearlite (black phase) and ferrite (white phase), respectively. Moreover, ferrite distributes in strips parallel to the rolling direction with pearlite and the volume fraction of ferrite is approximately 60%. However, the banded structure is a common microstructural defect in the process of casting and hot rolling, which is caused by the differential diffusion rates of carbon and impurity elements dissolved in austenite. It severely affects the subsequent processing and performance of steel materials [24-25].

3.2. Statistical results of ferrite grain size

3.2.1. Statistical results for interval length of 5 μm

For the 5 μm interval length, the statistical results both of the ferrite number percentage N_f and the ferrite area fraction density ρ_{Af} are presented in Figs. 4 and 5, respectively. Figs. 4 and 5 reveal the distribution rules of ferrite grain size are almost

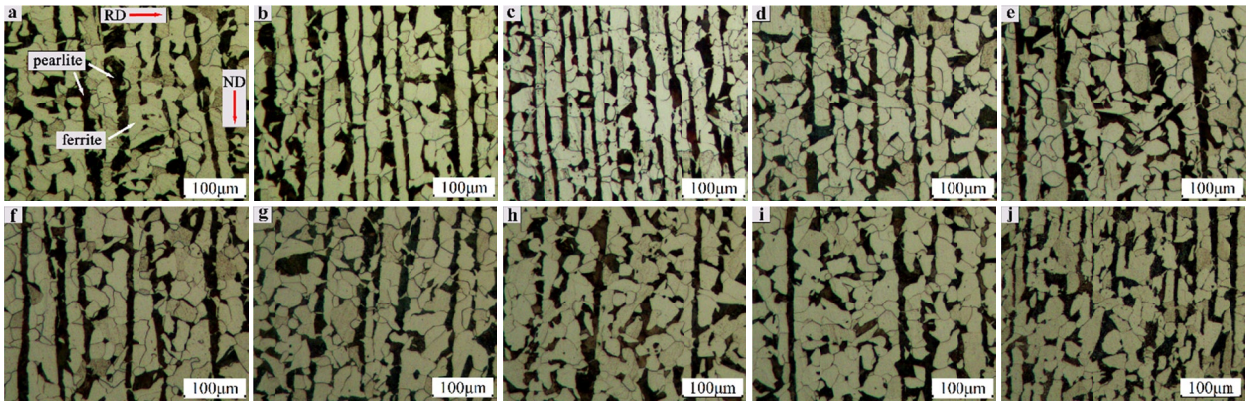

Fig. 3. Typical microstructure of different post-fire test pieces (a) 20℃-0 min; (b) 300℃-40 min; (c) 500℃-40 min; (d) 700℃-40 min; (e) 300℃-60 min; (f) 500℃-60 min; (g) 700℃-60 min; (h) 300℃-120 min; (i) 500℃-120 min; (j) 700℃-120 min

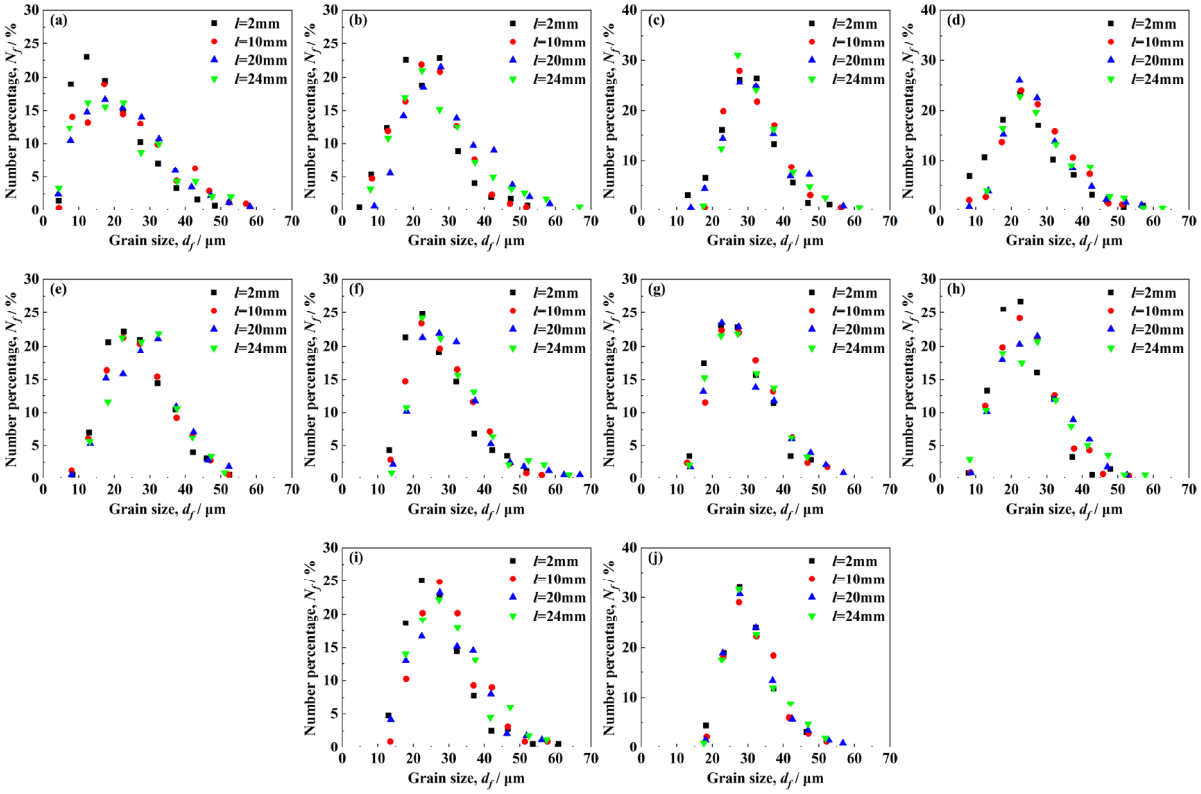

Fig. 4. Number percentage N_f of ferrite grain in the investigated 40 mm-thick Q345 steel under different fire environments (a) N_f-20℃-0 min; (b) N_f-300℃-40 min; (c) N_f-500℃-40 min; (d) N_f-700℃-40 min; (e) N_f-300℃-60 min; (f) N_f-500℃-60 min; (g) N_f-700℃-60 min; (h) N_f-300℃-120 min; (i) N_f-500℃-120 min; (j) N_f-700℃-120 min

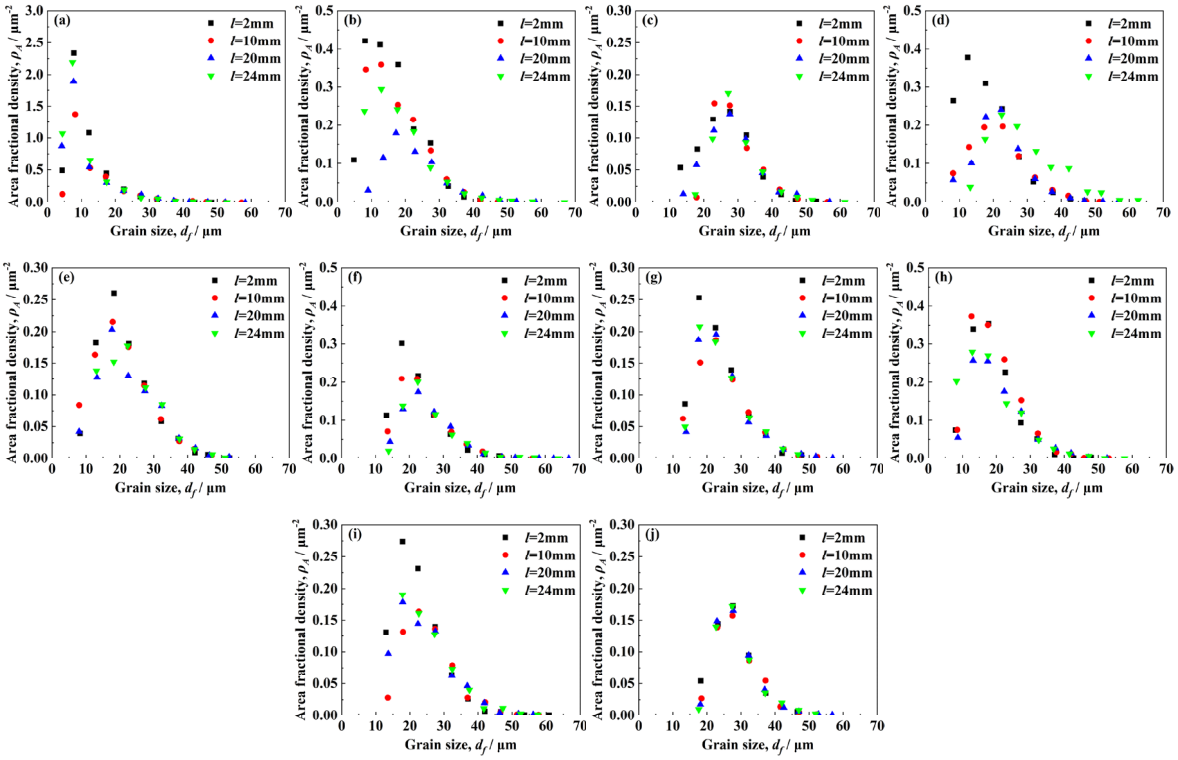

Fig. 5. Area fraction density ρ_{Af} of ferrite grain in the investigated 40 mm-thick Q345 steel under different fire environments (a) ρ_{Af}-20℃-0 min; (b) ρ_{Af}-300℃-40 min; (c) ρ_{Af}-500℃-40 min; (d) ρ_{Af}-700℃-40 min; (e) ρ_{Af}-300℃-60 min; (f) ρ_{Af}-500℃-60 min; (g) ρ_{Af}-700℃-60 min; (h) ρ_{Af}-300℃-120 min; (i) ρ_{Af}-500℃-12 0 min; (j) ρ_{Af}-700℃-120 min

the same at four different locations (l = 2 mm, 10 mm, 20 mm and 24 mm) under different fire temperatures, but the peak point of ferrite grain size distribution is different under different fire temperatures. As the ferrite grain size d_f increases, both N_f and ρ_{Af} first increase and then decrease. A logarithmic normal distribution is observed between N_f and d_f, as well as between ρ_{Af} and d_f. Moreover, there is a notable lack of uniformity in distribution of the ferrite grain size.

3.2.2. Statistical results for interval lengths of 3 μm and 10 μm

By employing two different interval lengths of 3 μm and 10 μm, statistical analysis was performed on the ferrite grain size in Q345 thick plates for various fire temperatures. Due to the influence of interval length L on N_f or ρ_{Af} is basically the same under different fire conditions, the statistical results under the fire conditions of 700℃-120 min were selected as a representative example and were analyzed, as illustrated in Fig. 6.

From Fig. 6, it is evident that the distribution of ferrite grain size exhibits greater dispersion and has poor continuity in distribution when a 10μm interval length is employed. Conversely, when a 3 μm interval length is utilized, the ferrite grain size is more densely distributed. Consequently, the selection of interval length significantly influences the description of the non-uniform distribution of ferrite grain size in Q345 thick plates.

4. Analysis and discussion

Based on the non-uniform distribution of ferrite grain size in Q345 thick plates, a Log-Normal logarithmic function given in Equation (5) is used to fit the statistical results [26]. Taking the 5 μm-length interval as an example, the relationships between the average diameter d_f both and the proportion of ferrite

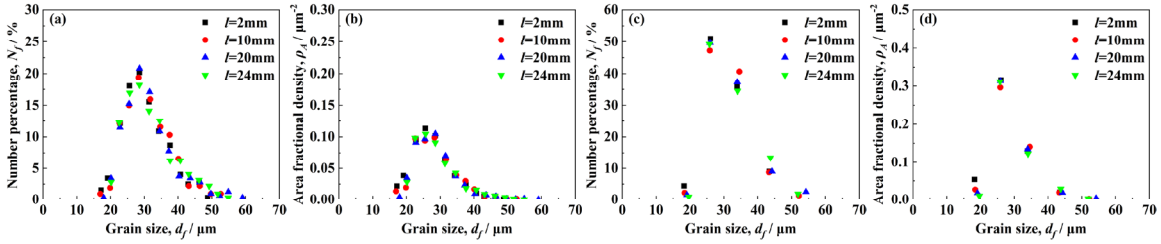

Fig. 6. Statistical results both of ferrite grain distribution parameters N_f and ρ_{Af} with two different interval lengths of 3 μm and 10 μm under the fire conditions of 700℃-120 min (a) N_f-700℃-120 min-3 μm; (b) ρ_{Af}-700℃-120 min-3 μm; (c) N_f-700℃-120 min-10 μm; (d) ρ_{Af}-700℃-120 min-10 μm

grain quantity N_f and the area fraction density ρ_{Af} were studied for different fire environments. Additionally, the influence of interval length L on the accuracy of the non-uniform distribution model is examined.

$$y = y_0 + \frac{A}{\sqrt{2\pi}\omega x} e^{\frac{-\left[\ln\frac{x}{xc}\right]^2}{2\omega^2}} \tag{5}$$

where y_0 is the offset, A is the peak area, ω is the standard deviation in logarithmic scale, and x_c is the center position.

4.1. Non-uniform distribution model of ferrite grain quantity proportion (N_f)

To assess the distribution pattern of the ferrite grain percentage N_f relative to the average diameter d_f, Equation (5) was employed to fit the relationships between N_f and d_f under different fire environments, and the fitting results are presented in Fig. 7, Equation (6) and TABLE 3, respectively.

$$N_f = N_{f0} + \frac{A}{\sqrt{2\pi}\omega d_f} e^{\frac{-\left[\ln\frac{d_f}{dc}\right]^2}{2\omega^2}} \tag{6}$$

where N_f is the number percentage of ferrite grains within each statistical interval, %; N_{f0} is the offset, %; A is the peak area, %·μm; ω is the standard deviation in logarithmic scale, μm; d_c is the center position, μm.

Based on Fig. 7, it can be observed that there exists a quantitative relationship between N_f and d_f following a Log-Normal function. From TABLE 3, there is no significant relationship between fire temperature T and N_{f0}, T and A, T and ω, T and d_c. The change range of each parameter is –6.80% ~ 19.43% for N_{f0}, 368.20% · μm ~ 1682.56% · μm for A, 0.18 μm ~ 0.97 μm for ω, and 19.69 μm ~ 39.28 μm for d_c, respectively. Their reliabilities of these models are indicated by their determination coefficients R^2, Notably, when subjected to a service temperature of 300°C for 60 minutes, the minimum value of R^2 is 0.8519. Therefore, these N_f-d_f empirical models can accurately describe and predict the variation trend of the non-uniform distribution of ferrite grain size in Q345 thick plates after exposure to fire. Base on which we can thereby achieve microstructural optimization and performance improvement of the material [27-28].

4.2. Non-uniform distribution model of ferrite grain area fraction density (ρ_{Af})

To quantitatively describe the relationship between the ferrite grain area fraction density ρ_{Af} and the average diameter d_f, the distribution pattern of ρ_{Af} was fitted by using Equation (5) under different fire environments. The fitting results are presented in Equation (7), Fig. 8 and TABLE 4, respectively.

$$\rho_{Af} = \rho_{f0} + \frac{A}{\sqrt{2\pi}\omega d_f} e^{\frac{-\left[\ln\frac{d_f}{dc}\right]^2}{2\omega^2}} \tag{7}$$

where ρ_{Af} is the ferrite grain area fraction density within each statistical interval, μm^{-2}; ρ_{f0} is the offset, μm^{-2}; A is the peak

TABLE 3

The fitting results of each parameter in the N_f-d_f empirical model given in Equation (6)

Test condition	Log-Normal parameters											
	l/mm	N_{f0}, %	A, %·μm	ω, μm	d_c, μm	R^2	l/mm	N_{f0}, %	A, %·μm	ω, μm	d_c, μm	R^2
20°C-0 min	2	–3.5487	705.4547	0.6613	19.6879	0.9724	20	–6.8015	1128.9001	0.8603	31.7870	0.9448
300°C-40 min		0.0636	494.4173	0.4023	22.9455	0.8620		–0.2720	517.5035	0.3854	28.2384	0.9473
500°C-40 min		1.8477	406.4525	0.2086	30.0643	0.9572		1.6534	412.7679	0.2199	30.9006	0.9655
700°C-40 min		1.4816	413.9532	0.3692	23.2578	0.9092		1.1917	421.0299	0.2754	25.6090	0.9937
300°C-60 min		–0.9631	558.7611	0.3807	26.0224	0.9861		–0.7802	553.1091	0.3872	29.1192	0.8519
500°C-60 min		0.8405	443.7017	0.3105	24.6587	0.9578		0.2326	461.6222	0.2827	28.6035	0.9831
700°C-60 min		–3.0296	631.6528	0.3617	27.3614	0.9591		0.6191	457.6017	0.3030	27.2020	0.9538
300°C-120 min		–0.2185	492.5270	0.3352	22.2256	0.9743		–2.0882	612.1204	0.4304	26.3474	0.9591
500°C-120 min		0.1362	478.5128	0.3056	25.3358	0.9925		–1.9199	586.9196	0.3710	29.5683	0.9128
700°C-120 min		2.9451	368.1961	0.1783	29.1172	0.9969		1.0901	428.1209	0.2013	29.4389	0.9879
20°C-0 min	10	11.2080	1682.5568	0.9726	39.2792	0.9005	24	–5.3749	959.4399	0.8537	28.8609	0.9172
300°C-40 min		–0.3619	515.8737	0.4073	24.8598	0.8723		0.8857	442.6113	0.4112	24.7532	0.9779
500°C-40 min		–1.6756	564.4344	0.2589	30.8870	0.9507		1.4573	433.8282	0.2019	30.4758	0.9545
700°C-40 min		0.7026	462.8025	0.3130	26.8713	0.9753		0.3202	472.1148	0.3466	26.5800	0.9604
300°C-60 min		–0.0152	501.4579	0.3671	26.7094	0.9875		1.0268	458.2706	0.2997	28.3962	0.8911
500°C-60 min		–1.7532	571.0388	0.3544	27.8959	0.9762		0.6396	447.7594	0.2878	27.8974	0.9457
700°C-60 min		–0.4626	515.2891	0.3185	28.5433	0.9828		19.4347	1675.2535	0.5520	34.0423	0.9710
300°C-120 min		–1.3131	561.7283	0.3834	24.3511	0.9639		–0.7567	540.5328	0.4386	25.5359	0.9326
500°C-120 min		0.0312	478.3653	0.2816	28.7294	0.9603		–0.5645	542.4017	0.3548	28.8467	0.9323
700°C-120 min		–0.8567	506.9499	0.2328	30.4790	0.9440		2.5258	387.8425	0.1902	29.1741	0.9469

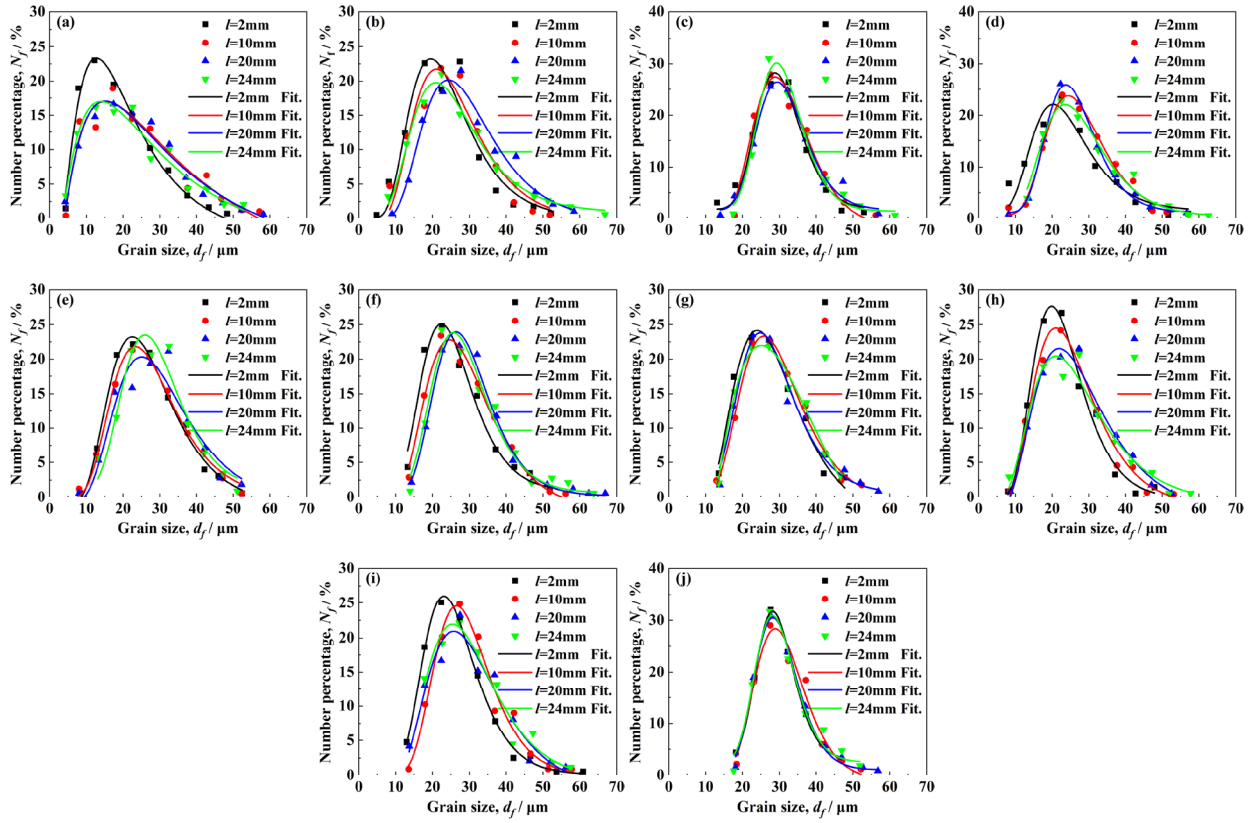

Fig. 7. The relationships between the proportion of ferrite grain number N_f and the average diameter d_f of the 40 mm-thick Q345 steel under different fire environments (a) N_f-20℃-0 min; (b) N_f-300℃-40 min; (c) N_f-500℃-40 min; (d) N_f-700℃-40 min; (e) N_f-300℃-60 min; (f) N_f-500℃-60 min; (g) N_f-700℃-60 min; (h) N_f-300℃-120 min; (i) N_f-500℃-120 min; (j) N_f-700℃-120 min

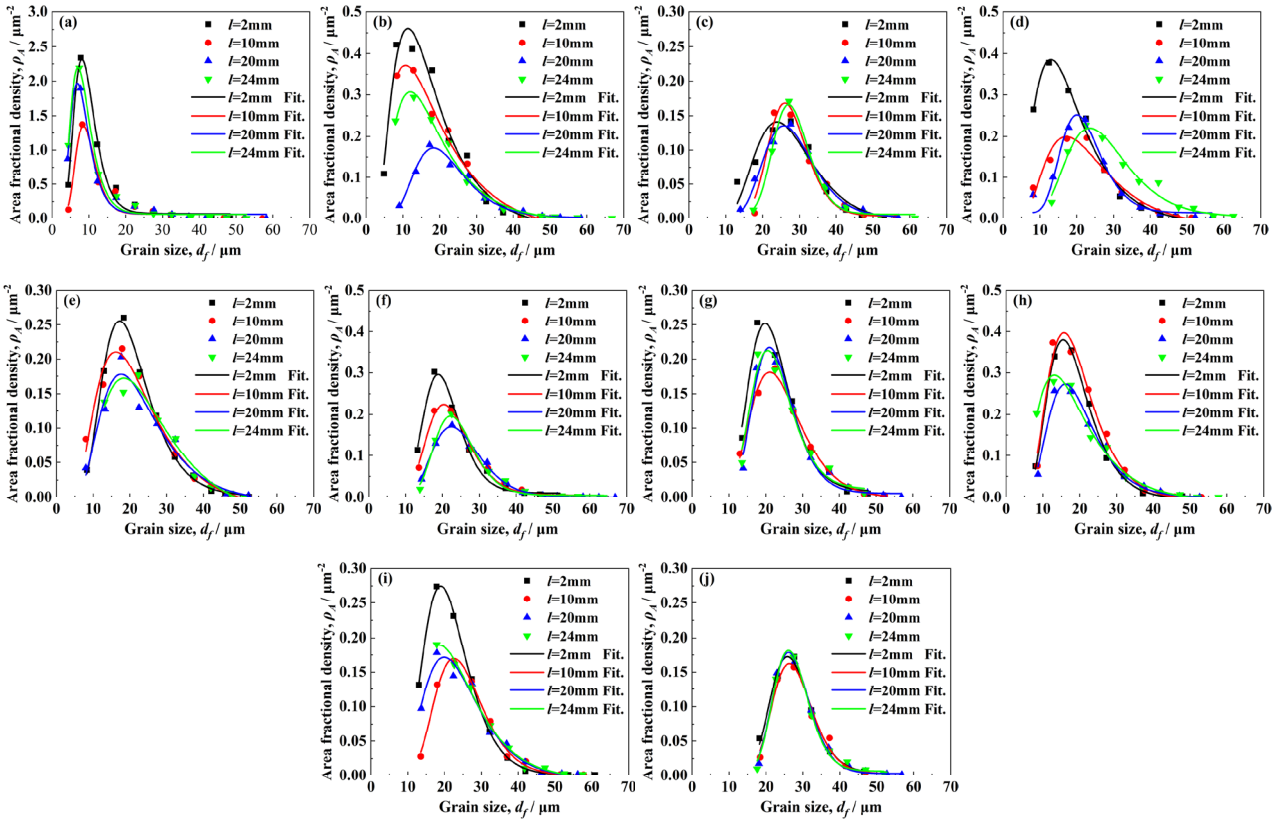

Fig. 8. The relationships between the ferrite grain area fraction density ρ_{Af} and the average diameter d_f of the 40 mm-thick Q345 steel under different fire environments (a) ρ_{Af}-20℃-0 min; (b) ρ_{Af}-300℃-40 min; (c) ρ_{Af}-500℃-40 min; (d) ρ_{Af}-700℃-40 min; (e) ρ_{Af}-300℃-60 min; (f) ρ_{Af}-500℃-60 min; (g) ρ_{Af}-700℃-60 min; (h) ρ_{Af}-300℃-120 min; (i) ρ_{Af}-500℃-120 min; (j) ρ_{Af}-700℃-120 min

TABLE 4

The fitting results of each parameter in the ρ_{Af}-d_f empirical model given in Equation (7)

Test condition	Log-Normal parameters											
	l/mm	ρ_{f0}, μm^{-2}	A, μm^{-2}·μm	ω, μm	d_c, μm	R^2	l/mm	ρ_{f0}, μm^{-2}	A, μm^{-2}·μm	ω, μm	d_c, μm	R^2
20°C-0 min	2	0.0699	16.7475	0.3461	9.1283	0.9795	20	0.0631	12.9931	0.3709	7.8668	0.9763
300°C-40 min		–0.0257	9.2630	0.5691	15.6940	0.9639		0.0016	3.0598	0.3664	20.9480	0.9805
500°C-40 min		–0.0047	3.0112	0.3264	26.6170	0.8528		0.0018	2.3048	0.2576	27.5633	0.9704
700°C-40 min		–0.0151	7.7196	0.5188	16.9463	0.9870		0.0137	3.3384	0.2687	21.5635	0.9548
300°C-60 min		0.0014	4.2114	0.3599	19.5828	0.9942		0.0062	3.9858	0.4449	21.4519	0.9293
500°C-60 min		0.0104	3.5619	0.2560	20.1148	0.9815		0.0003	2.7870	0.2813	24.2560	0.9923
700°C-60 min		0.0088	3.4284	0.2737	21.3413	0.9565		0.0058	2.9140	0.2541	22.3708	0.9682
300°C-120 min		–0.0042	5.7421	0.3610	17.6282	0.9954		0.0005	4.5283	0.3821	18.6196	0.9761
500°C-120 min		–0.0003	4.2684	0.3115	20.8731	0.9984		0.0048	3.5389	0.3751	22.8886	0.9636
700°C-120 min		0.0036	2.3144	0.2073	26.9417	0.9787		0.0029	2.1875	0.1868	27.0471	0.9881
20°C-0 min	10	0.0632	8.7036	0.3032	9.2930	0.9195	24	0.0606	15.3571	0.3801	8.1175	0.9853
300°C-40 min		–0.0414	9.6707	0.6883	17.2083	0.9863		0.0092	6.2896	0.5647	16.5110	0.9905
500°C-40 min		0.0037	2.1530	0.1968	27.0919	0.9293		0.0061	1.9508	0.1775	27.9160	0.9844
700°C-40 min		–0.0208	5.2861	0.4936	21.9133	0.9312		0.0032	4.7212	0.3466	26.5800	0.9604
300°C-60 min		–0.0169	5.1590	0.4959	20.6594	0.9683		0.0300	5.3033	0.5033	23.5994	0.9497
500°C-60 min		0.0053	3.2028	0.2759	21.9725	0.9829		0.0052	2.5703	0.2350	23.4927	0.9782
700°C-60 min		–0.0010	3.2510	0.3214	23.3906	0.9881		0.0117	2.8287	0.2645	22.0003	0.9354
300°C-120 min		–0.0067	6.5605	0.3836	18.1977	0.9732		0.0103	5.9987	0.5237	17.2358	0.9828
500°C-120 min		–0.0010	2.8751	0.2861	24.4488	0.9883		0.0058	4.0497	0.4097	21.9860	0.9906
700°C-120 min		0.0025	2.1699	0.2018	27.4039	0.9691		0.0064	2.0716	0.1779	26.9306	0.9834

area, μm^{-2}·μm; ω is the standard deviation in logarithmic scale, μm; d_c is the center position, μm;

From TABLE 4, parameters ρ_{f0}, A, ω, and d_c differ obviously in their values under different fire temperature T. the variation range is from –0.04 μm^{-2} to 0.07 μm^{-2} for ρ_{f0}, from 1.95 μm^{-2}·μm to 16.75 μm^{-2}·μm for A, from 0.18 μm to 0.69 μm for ω, and from 7.87 μm to 27.56 μm for dc, respectively. Moreover, the minimum value of R^2 is 0.8528 under the fire conditions of 500°C-40 min. This indicates that these ρ_{Af}-d_f empirical models can effectively characterize the distribution of ferrite grain size. Furthermore, the utilization of Equation (7) enables accurate prediction of the fluctuations in ferrite grain size of the investigated material.

4.3. The influence of short-term high temperature service environment on ferrite grain distribution

4.3.1. The influence of fire temperature on nonuniformity distribution of ferrite grain size

In order to investigate the influence of fire temperature T on the non-uniform distribution of ferrite grain in Q345 steel, the relationships between the fire temperature T and both the peak points (d_{fN}, $N_{f\max}$) and ($d_{f\rho}$, $\rho_{Af\max}$) of the non-uniform distribution models expressed in Equations (6) and (7) are discussed. Considering that the influence of fire temperature T on the non-uniform distribution of ferrite grain in Q345 steel is essentially the same for different locations with l = 2 mm, l = 10 mm, l = 20 mm and l = 24 mm, respectively. The results of non-uniform distribution at location with l = 20 mm is considered as the general results given in Fig. 9, and is employed to discuss the influence of fire temperature on nonuniformity distribution of ferrite grain.

According to Figs. 9a-9c, it can be observed that different fire temperatures result in different values of d_{fN}, and $N_{f\max}$ generally increases with the increase of fire temperature T when the fire duration is the same. The range of d_{fN} variations under three different fire durations are 15.15 μm ~ 25.30 μm for 40 min, 15.15 μm ~ 26.39 μm for 60 min, and 15.15 μm ~ 29.94 μm for 120 min, respectively. Compared to room temperature, the maximum increase of $N_{f\max}$ under the three fire durations is 55.30% (40 min), 40.30% (60 min) and 131.70% (120 min), respectively. Figs. 9d-9f show that fire temperature leads to a sharp decrease in $\rho_{Af\max}$ value and an increase in $d_{f\rho}$. From the above results, it can be concluded that the fire temperature T significantly affects the non-uniform distribution of ferrite grain size in the 40 mm-thick Q345 steel.

4.3.2. The influence of fire duration on the non-uniform distribution of ferrite grain size

Similarly, taking the non-uniform distribution results at the location with l = 20 mm as the general result, the relationships between the fire duration t and both the peak points (d_{fN}, $N_{f\max}$) and ($d_{f\rho}$, $\rho_{Af\max}$) of above mentioned non-uniform distribution models given in Equations (6) and (7) are discussed. The results are presented in Fig. 10.

Based on Figs. 10a-10c, it can be observed that different fire durations result in different values of d_{fN}, and $N_{f\max}$ generally increases under the same fire temperature. Under three differ-

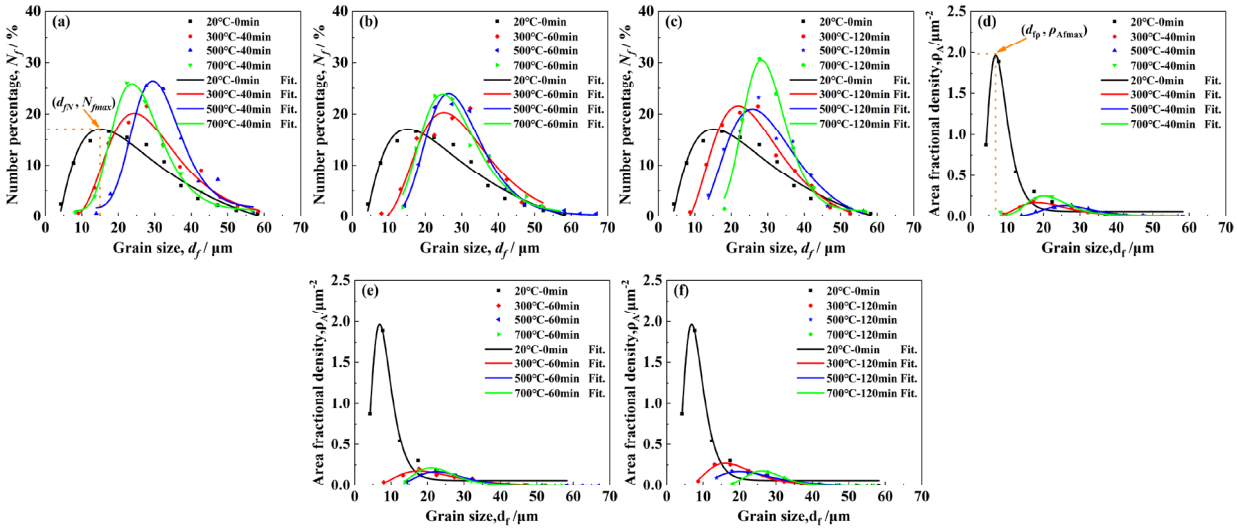

Fig. 9. The influence of fire temperature T on the non-uniform distribution of ferrite grain size in the 40 mm-thick Q345 steel (a) N_f-40 min; (b) N_f-60 min; (c) N_f-120 min; (d) ρ_{Af}-40 min; (e) ρ_{Af}-60 min; (f) ρ_{Af}-120 min

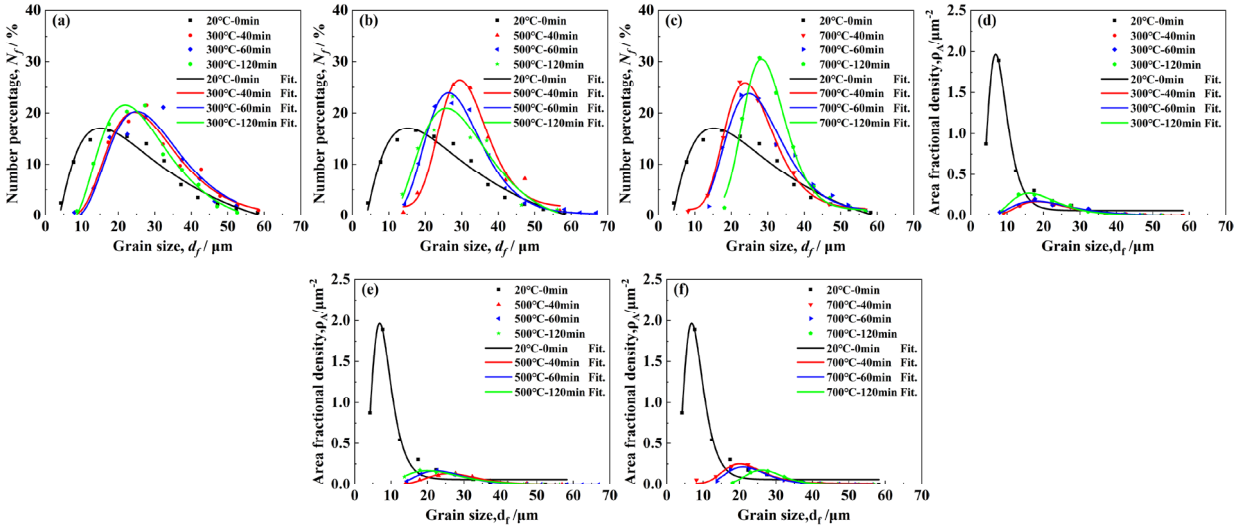

Fig. 10. The impact of fire duration on non-uniform grain distribution (a) N_f-300°C; (b) N_f-500°C; (c) N_f-700°C; (d) ρ_{Af}-300°C; (e) ρ_{Af}-500°C; (f) ρ_{Af}-700°C

ent fire temperatures, $N_{f\max}$ varies from 17.05% to 21.53% for 300°C, from 17.05% to 26.48% for 500°C and from 17.05% to 30.50% for 700°C, respectively. The range of d_{fN} variations is as follows: 15.15 μm to 25.10 μm (300°C), 15.15 μm to 29.43 μm (500°C), and 15.15 μm to 28.27 μm (700°C). Figs. 10d-10f demonstrate that fire duration leads to a sharp decrease in the value of $\rho_{Af\max}$ and an increase in that of $d_{f\rho}$. In conclusion, fire duration t has significant effect on the non-uniform distribution of ferrite grain size in the 40 mm-thick Q345 steel.

4.4. Comparison of ferrite grain size in the thickness direction under different fire environments

To reveal the effect of fire environment on the grain size of ferrite in the investigated Q345 heavy plate, the average diameter d of all ferrite grains with the same distance l is determined by calculating the mean of the individual grain diameters d_i. When the distance l is separately equal to 2 mm, 10 mm, 20 mm and 24 mm, the statistical results of the average diameter d are illustrated in Fig. 11.

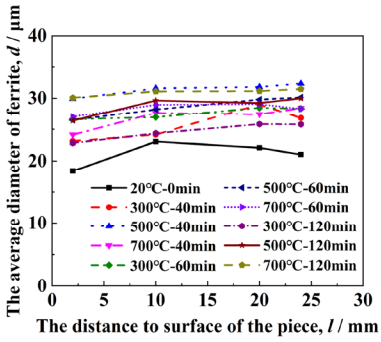

Fig. 11. Statistical results of the average diameter d of ferrite grains in the investigated Q345 heavy plate under different fire environments

Fig. 11 demonstrates that the ferrite diameter d initially increases and then decreases when the distance l changes from 2 mm to 20 mm under the condition of 20°C-0 min. However, the ferrite diameter d of different post-fire samples all exhibits a slow growth trend with an increase ranging from approximately 4% to 20%.

4.5. The influence of interval length L on the accurate description of the non-uniform distribution of ferrite grain size

4.5.1. Comparison of statistical results of ferrite grain size with different interval lengths

In order to elucidate the impact of interval length on the accuracy of statistical analysis of the non-uniform distribution of ferrite grain size, the non-uniform distribution of ferrite grain size at the location with l = 20 mm under the fire conditions of 700°C-120 min were subjected to statistical analysis using three different interval lengths (L = 3 μm, 5 μm and 10 μm), as shown in Fig. 12 and TABLE 5, respectively.

According to the data presented in TABLE 5, it is evident that the fitting results of R^2 with three different interval lengths are significantly different. The fitting accuracy of the interval length with 5 μm is better than that of the other two interval lengths for the two distribution parameters N_f and ρ_{Af}. However, the worst fitting results are obtained from the longest interval with 10 μm, because the longer the interval, the smaller the number of ferrite samples. Furthermore, the longer the interval, the more dispersed the ferrite distribution is. Thus, the interval length exerts a discernible influence on the statistical accuracy of the non-uniform distribution of grain size.

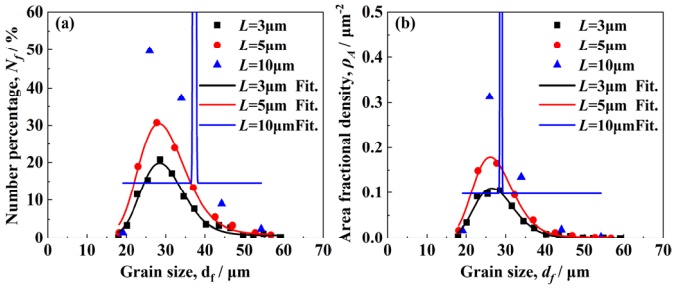

Fig. 12. The influence of interval length on the statistical accuracy of ferrite grain size at the location with l = 20 mm under the fire conditions of the 700°C-120 min (a) N_f-700°C-120 min; (b) ρ_{Af}-700°C-120 min

4.5.2. Analysis on the reasonable range for the interval length L

According to section 4.5.1, the statistical accuracy of the ferrite grain size distribution is influenced by the interval length, and a higher statistical accuracy is obtained when the interval length L is equal to 5 μm. In order to determine an appropriate interval length efficiently, both the average diameter d and the ration of d to L were calculated for each experimental condition. The calculated results are presented in TABLE 6, which indicate that the ratio of d to L changes from 4 to 6. Therefore, it is recommended to use an interval length of 5 μm so as to improve statistical accuracy.

TABLE 5

The fitting results of R^2 in Fig. 12

Distance to the surface l/mm	Interval length L/μm	The number percentage of ferrite grain N_f/%	Ferrite area fraction density ρ_{Af}/μm^{-2}
20	3	0.9746	0.9753
	5	0.9879	0.9881
	10	–3.2973	–3

TABLE 6

Statistical results of the average diameter d and the ratio of d to L for each fire condition (L = 5 μm)

Test condition	l = 2 mm		l = 10 mm		l = 20 mm		l = 24 mm	
	d/μm	d/L	d/μm	d/L	d/μm	d/L	d/μm	d/L
20°C-0 min	18	4	23	5	22	4	21	4
300°C-40 min	23	5	24	5	29	6	27	5
500°C-40 min	30	6	32	6	32	6	32	6
700°C-40 min	24	5	28	6	27	5	28	6
300°C-60 min	27	5	27	5	28	6	28	6
500°C-60 min	26	5	28	6	30	6	30	6
700°C-60 min	27	5	29	6	29	6	28	6
300°C-120 min	23	5	24	5	26	5	26	5
500°C-120 min	26	5	30	6	29	6	30	6
700°C-120 min	30	6	31	6	31	6	31	6

5. Conclusions

(1) Under various fire environments, the distribution rules of ferrite grain size are almost the same at four different locations with l = 2 mm, l = 10 mm, l = 20 mm and l = 24 mm, respectively. With increasing the ferrite grain size d_f, both the number percentage of ferrite N_f and the ferrite area fraction density ρ_{Af} initially increase sharply, then decrease significantly and stabilizes. This reveals that the distribution of ferrite grain size is non-uniform in the 40 mm-thick Q345 steel.

(2) The relationships between N_f and d_f, as well as between ρ_{Af} and d_f, follow the logarithmic normal distribution law. For each fire environments, the N_f- d_f empirical model and the ρ_{Af}-d_f empirical model were separately proposed by using a reasonable interval length of 5 μm. These models can accurately describe and predict the trend of grain size changes in the investigated Q345 heavy plate because the fitting results of their R^2 are all larger than 0.85. This is of great significance for material preparation and performance regulation.

(3) Both the fire temperature T and the fire duration t have significant impact on the distribution of ferrite grain size in the thickness direction. When the fire duration t remains constant, $N_{f\max}$, d_{fN} and $d_{f\rho}$ increase with the rise of fire temperature T, and the minimum increment of $N_{f\max}$ is about 40.3%. However, $\rho_{Af\max}$ decreases sharply with increasing the fire temperature T. When the fire temperature T is the same, both $N_{f\max}$ and d_{fN} change obviously with changing the fire duration t. Furthermore, the fire duration leads to a sharp decrease in the value of $\rho_{Af\max}$ and an increase in that of $d_{f\rho}$.

(4) The interval length L has a significant impact on the statistical accuracy of non-uniform distribution of grain size. The ratio of L to the grain diameter d can be used to determine a reasonable interval length. For the employed 40 mm-thick Q345 steel, the reasonable interval length is about 4 to 6 times the grain diameter d. Obviously, the determination of reasonable interval length is of great significance for studying the non-uniform distribution of grains.

Acknowledgements

This work was funded by Anhui University Science Research Projects (2022AH051630, KJ2021A0862 and KJ2021ZD0111), Anhui Market Bureau Science and Technology Plan Project (2021MK034) and Bengbu Technology Plan Project (2022hm06), respectively.

REFERENCES

[1] C. Zhang, R.H. Wang, L. Zhu, Mechanical properties of Q345 structural steel after artificial cooling from elevated temperatures [J]. Journal of Constructional Steel Research **176**, 106432 (2021).

[2] G. Shi, S.H. Wang, C.X. Rong. Experimental investigation into mechanical properties of Q345 steel after fire [J]. Journal of Constructional Steel Research **199**, 107582 (2022).

[3] W.J. Dan, R.B. Gou, M. Yu, et al., Experimental study on the post-fire mechanical behaviours of structural steels [J]. Journal of Constructional Steel Research **199**, 107629 (2022).

[4] W. Yu, G.S. Li, Q.W. Cai, Effect of a novel gradient temperature rolling process on deformation, microstructure and mechanical properties of ultra-heavy plate [J]. Journal of Materials Processing Technology **217**, 317-326 (2015).

[5] L.Z. Xu, G.Y. Qiao, X. Gong, et al., Effect of through-thickness microstructure inhomogeneity on mechanical properties and strain hardening behavior in heavy-wall X70 pipeline steels [J]. Journal of Materials Research and Technology **25**, 4216-4230 (2023).

[6] C.T. Zhang, M.Q. Gong, L. Zhu, Post-fire mechanical behavior of Q345 structural steel after repeated cooling from elevated temperatures with fire-extinguishing foam [J]. Journal of Constructional Steel Research **191**, 107201 (2022).

[7] W. Li, H. Chen, Hysteretic performance of structural steels after exposure to elevated temperatures [J]. Thin-Walled Structures **191**, 111019 (2023).

[8] M.L. Lobanov, M.L. Krasnov, V.N. Urtsev, et al., Effect of cooling rate on the structure of low-carbon low-alloy steel after thermomechanical controlled processing [J]. Metal Science and Heat Treatment **61**, 32-38 (2019).

[9] K. Pańcikiewicz, M. Maślak, M. Pazdanowski, et al., Changes in the microstructure of selected structural alloy steel grades identified after their simulated exposure to fire temperature [J]. Case Studies in Construction Materials **18**, e01923 (2023).

[10] Z.Y. Chen, X.J. Zhao, J.J. Qi, et al., Effect of tempering on the microstructure and properties of a new multi-functional 460 MPa Grade construction structural steel [J]. Journal of Materials Research and Technology **18**, 1092-1104 (2022).

[11] X. Xue, Y. Shi, X. Zhou, et al., Experimental study on the properties of Q960 ultra-high-strength steel after fire exposure [J]. Structures **47**, 2081-2098 (2023).

[12] X. Zeng, W.B. Wu, J.S. Huo, et al., Residual mechanical properties of Q890 high-strength structural steel after exposure to fire [J]. Construction and Building Materials **304**, 124661 (2021).

[13] L. Wang, C.R. Gao, Y.F. Wang, et al., Effect of thermomechanical controlled processing parameters on microstructure and properties of Q460q steel [J]. Journal of Iron and Steel Research International **17** (1), 38-43 (2010).

[14] X.Y. Wu, H.T. Lin, W. Luo, et al., Microstructure and microhardness evolution of thermal simulated HAZ of Q&P980 steel [J]. Journal of Materials Research and Technology **15**, 6067-6078 (2021).

[15] D.C. Wan, W. Yu, X.L. Li, et al., Effect of quenching temperature on microstructure and mechanical properties of 550 MPa grade thick steel plate [J]. Acta Metallurgica Sinica **48** (5), 455-460 (2012). (in Chinese)

[16] S. Liu, S.Y. Ai, M.J. Long, et al., Evolution of microstructures and mechanical properties of Nb-V alloyed ultra-high strength hot stamping steel in austenitizing process [J]. Materials **15** (22), 8197 (2022).

[17] C.C. Li, S.L. Xie, Microstructure and properties of hot stamping boron steel using heated dies under different holding time [J]. Vacuum **170**, 108960 (2019).

[18] Z.J. Xie, Y.P. Fang, Y. Cui, et al., Effect of reheating rate on microstructure and properties of high-strength-toughness steel [J]. Materials Science and Technology **32** (7), 691-696 (2016).

[19] M. Yu, R.B. Gou, W.J. Dan, et al., Microstructure Distribution Parameters for Ferrite-Martensite Dual-Phase Steel [J]. Strength of Materials **53** (1), 173-182 (2021).

[20] A.A. Kazakov, D.V. Kiselev, O.V. Sych, et al., Quantitative assessment of microstructural inhomogeneity by thickness of hot-rolled plates made of cold-resistant low-alloy steel for Arctic applications [J]. CIS Iron and Steel Review **20**, 41-49 (2020).

[21] T. Amashita, K. Ushioda, H. Fujii, Inhomogeneity of microstructure along the thickness direction in stir zone of friction stir welded duplex stainless steel [J]. ISIJ International 192 (2023).

[22] B. Virgínia, Q.X. Jiang, S. Scholl, et al., A comprehensive quantitative characterisation of the multiphase microstructure of a thick-section high strength steel [J]. Journal of Materials Science **57** (13), 7101-7126 (2022).

[23] X.D. Huang, M.H. Zhou, T.Y. Zhang, et al., Effect of Banded Structure on the Cr-Ni-Mo-V Steel High-Temperature Frictional and Wear Performance [J]. Tribology Letters **71**, 58 (2023).

[24] J.H. Liang, Z.Z. Zhao, D. Tang, et al., Improved microstructural homogeneity and mechanical property of medium manganese steel with Mn segregation banding by alternating lath matrix [J]. Materials Science & Engineering A **711**,175-181 (2018).

[25] D. Bhattacharjee, J.F. Knott, C.L. Davis, Charpy-impact-toughness prediction using an "effective" grain size for thermomechanically controlled rolled microalloyed steels [J]. Metallurgical and Materials Transactions A **35**, 121-130 (2004).

[26] J.W. Park, K.S. Shin, Improved stretch formability of AZ31 sheet via grain size control [J]. Materials Science and Engineering A **688**, 56-61 (2017).